Fractographic Analyses of Fatigue Fracture Surfaces of 7050 Aluminium Alloy

R. GÜRBÜZ and M. DORUK* and W. SCHÜTZ**
*Metallurgical Engineering Department Middle East Technical University, 06531 Ankara, Turkey
**Industrieanlagen-Betriebsgesellschaft mbH., IABG, 8012 Ottobrunn, FRG

ABSTRACT

The fatigue-fracture surfaces of 7050 Al-alloy were investigated. 1" C-T specimens cut from a rolled plate of alloy at six different orientations were tested under fatigue loading. Two different environments, laboratory air and salt water fog were used in conducting the experiments. The examination of the fatigue crack propagation surfaces showed that the fracture was of transgranular type. Fatigue striations and secondary cracks were observed extensively on the fracture surfaces. The random formation of striations around intermetallic particles was explained by the existence of hydrogen embrittlement mechanism. Striations were observed at all crack growth rates between 10^{-4} and 10^{-2} mm/cycle, but their density, however, was found to decrease with increasing crack growth rate.

KEYWORDS

Corrosion fatigue; 7050 Al-alloy; Fatigue fracture surfaces.

INTRODUCTION

The corrosion fatigue properties of 7050 Al-alloy have gained great importance in recent years because of its extensive use in the form of plates in many components of primary load carrying structures of aircraft flying in marine atmospheres. Especially, military aircraft may continuously be exposed to splashing of sea water by wind or to salt water spray from the sea during their flight at low altitudes over the sea and during their taking off or landing on the deck of an aircraft carrier. In addition, the sea water which is condensed on the aircraft skin may cause the structural parts to be pre-exposed to aggressive sea water.

This work is a part of an extensive research (Gürbüz, 1987) on salt water enhanced fatigue crack growth behavior of 7050 T73651 Al-alloy. It aims at the discussion and characterization of the fracture behavior of this particular alloy through the SEM studies of fracture surfaces. For this purpose, 1" C-T specimens in six orientations (Fig. 1.) were first precracked. Following a pre-exposure in 5% NaCl solution, the specimens were placed into a special fog chamber, whereby they were subjected to a constant load amplitude (4900 N) sinusoidal wave with a frequency of 0.5 Hz at a stress ratio of R=0. A 5% NaCl solution acidified by H_2SO_4 to pH=4 was used for producing the fog. In order to have a basis of comprasion, some specimens were tested in the laboratory air under the same loading conditions except at the higher frequency of 2 Hz.

MICRO-STRUCTURE OF THE ALLOY

The testing material was a cold rolled plate of 7050 T73651 Al-alloy with the dimensions of 2000 x 1000 x 110 mm. The metallographic examinations showed that about one third of the microstructure was made up of recrystallized grains and two thirds of it consisted of polygonized grains. Very fine precipitates were observed to be evenly distributed throughout the structure, whereas larger intermetallic compounds (mostly $MgZn_2$ particles) were generally detected among the recrystallized grains (IABG, 1976). The flattening of the recrystallized grains in the short transverse (S) direction and their elongation in the rolling (L) direction were found to be significant.

MACRO-EXAMINATION OF FRACTURE SURFACES

The examination of the fracture surfaces of the failed specimens by eye and by low power magnifying glass showed a great dependency of surface textures on orientation. The fibrous appearance of the fracture surfaces in the rolling direction was apparent in all specimens except those with the loding direction being parallel to L.

All T-S and S-T specimens showed a strong texture in the thickness direction of the specimen which coincides with the rolling direction. The fibrous appearance of the surfaces in the longitudinal direction was, however, more pronounced in T-S as compared to S-T orientation.

A similar fibrous fracture surface appearance was observed in all S-L and T-L specimens with a strong texture in their crack growth direction, L. Such an appearance would not be expected in L-S and L-T specimens for which L was the loading direction.

The departure of the average through-thickness fatigue cracks from the plane of symmetry of the specimen was either absent or less than $\pm 5^o$ as recommended in ASTM E 647 (ASTM, 1980), for all orientations except L-S. L-S specimens showed a deviation of about 90^o from the initial crack plane presumably before the crack approaches its critical length. This deviation may be related to the microstructure and the stress state around the crack tip. The inspection of the fracture surface of L-S specimen both by SEM and by a low power microscope revealed the existence of large secondary cracks forming parallel to the crack front and growing perpendicular to the crack plane just before the deviation. These cracks can be thought to form between the layers formed by the elongated recrystallized grains and the polygonized

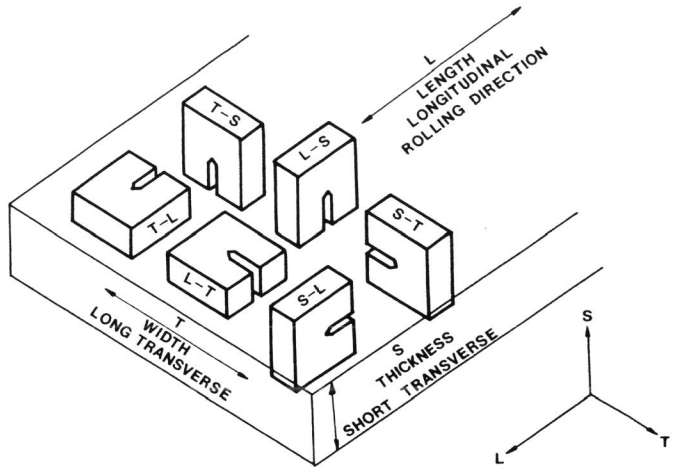

Fig. 1. The orientations of the C-T specimens in the rolled plate used in experiments.

grains between them. Since the deviation direction is parallel to the rolling direction, this may be a way to explain such a behavior. In addition, the change in the stress state at high crack lengths may form tensile stresses between the layers favoring the deviation.

45^o shear lips were observed on the fast fracture regions of the fracture surfaces of all specimens. Their size, however, showed a great variation depending on the specimen orientation. Largest shear lips observed on the fast fracture regions of L-S and L-T specimens suggest that their formation is favoured when the specimens are loaded in the rolling direction. Based on the layered structure, it can be concluded that larger shear lips form when the crack propagates perpendicular to those layers. The shear lips of T-S and T-L specimens were smaller in size as compared to those of L-S and L-T specimens.

It was observed that the curvature of the fatigue crack fronts in L-T, T-L, S-L and S-T specimens was slightly convex. This is probably because of the existence of plane-stress conditions at the free surfaces in front of the crack tip which restricts the propagation of the crack on specimen surfaces. Crack front curvature was almost linear in T-S orientation, because the layered structure of the alloy renders the crack front to be straight. The crack front curvature of L-S specimens, on the other hand, was observed to be concave.

SEM EXAMINATION OF FRACTURE SURFACES

The examination of fracture surfaces by scanning electron microscope, SEM, shows clearly that the crack propagation in air and salt water fog is of transgranular type and usually occurs along planes--with fatigue striations on them--joined by tear ridges. The mixed type of fracture that contains the intergranular cracks together with transgranular fracture planes with striations on them is encountered only in some regions of one of the S-L specimens tested in fog at high crack growth rates (Fig. 3b).

The tear ridges and furrows parallel to the crack growth direction observed on almost all specimens show that cracks propagate with several local fronts on different growth planes. Those local cracks with individual fronts then coalesce with each other as the macro crack extends. This coalescence takes place with ductile tearing between the planes of local cracks and thus forms tear ridges or furrows parallel to the local crack propagation direction. This phenomenon creates an apperance that resembles river patterns but is not really so (Figs. 2a and 5a).

Fatigue striations are observed extensively in all specimens at relatively lower and medium crack growth rates, on the transgranular planes separated by tear ridges or furrows (Figs. 2b, 5b and 6a). The density of the striations, however, decreases with increasing crack growth rate. Dimples, voids and void coalescence begin to appear together with striations at high ΔK values approaching the critical condition for crack instability (Figs. 3b and 7a). The curvature of the striations that shows the position of an advancing local crack front is always observed to be convex.

Figure 4a illustrates the random manner in which striations can form. This random formation of striations shows definitely that the growth direction of local crack fronts may be quite different than the macroscopic crack growth direction. The deviations leading to 120^{o} can be observed quite clearly in Fig. 4a. This fractograph probably shows some hydrogen diffusion around the inclusions or intermetallic particles causing the formation of microcracks at some distance ahead of the crack tip. These microcracks then propagate with the action of high tensile stresses leaving fatigue striations towards different directions before the main crack reaches those regions. Trapped hydrogen and the microcrack type analogy of the particles together with the high tensile stresses ahead of the crack tip, therefore, can trigger the hydrogen-induced cracking and the crack propagation observed around those particles (Duquette, 1982, Suresh et al., 1984).

The striations observed on fatigue fracture surfaces of all air fatigue specimens are of the ductile type. Whereas, brittle type of striations are sometimes found on some regions of the fracture surfaces of corrosion fatigue specimens. A good example of brittle striations can be seen in Fig. 7a.

Secondary cracks parallel to crack fronts and growing in a plane perpendicular to main crack growth plane are observed frequently in all specimens (Figs. 5b, 6b). They sometimes coalesce with each other and form longer secondary cracks. The coalescence of secondary cracks that seems to be texture dependent is extensively observed in T-S orientation where the secondary cracks are parallel to rolling direction. It is clearly apparent from the Figs. 5b and 6a that too many secondary cracks form between the

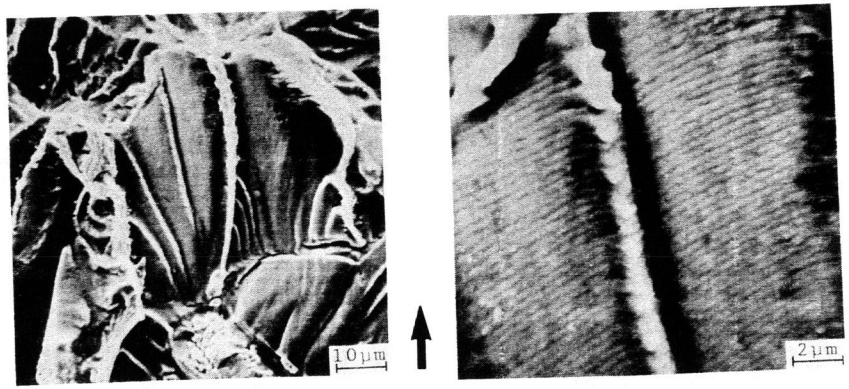

(a) (b)

Fig. 2. SEM fractographs
a) S-L in air, c.g.r. $\approx 2\times10^{-4}$ mm/cycle
b) S-L in air, c.g.r. $\approx 5\times10^{-4}$ mm/cycle
Arrow shows the crack growth direction.

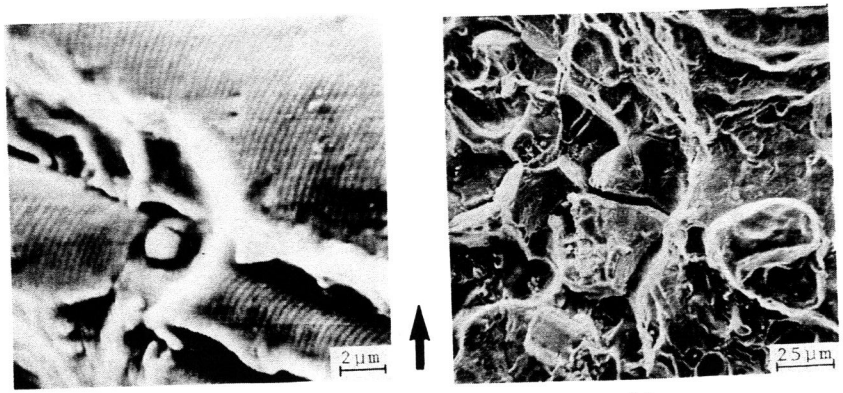

(a) (b)

Fig. 3. SEM fractographs
a) S-L in salt water fog, c.g.r. $\approx 3\times10^{-4}$ mm/cycle
b) S-L in salt water fog
Arrow shows the crack growth direction.

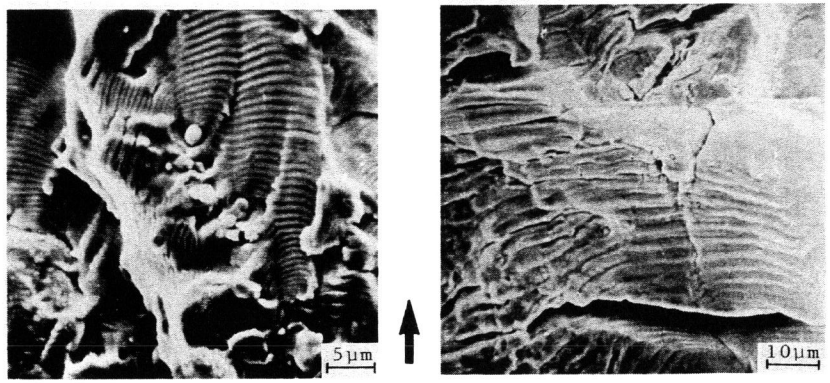

(a) (b)

Fig. 4. SEM fractographs
a) S-L in salt water fog, c.g.r. $\approx 8 \times 10^{-4}$ mm/cycle
b) L-T in air, c.g.r. $\approx 3 \times 10^{-3}$ mm/cycle
Arrow shows the crack growth direction.

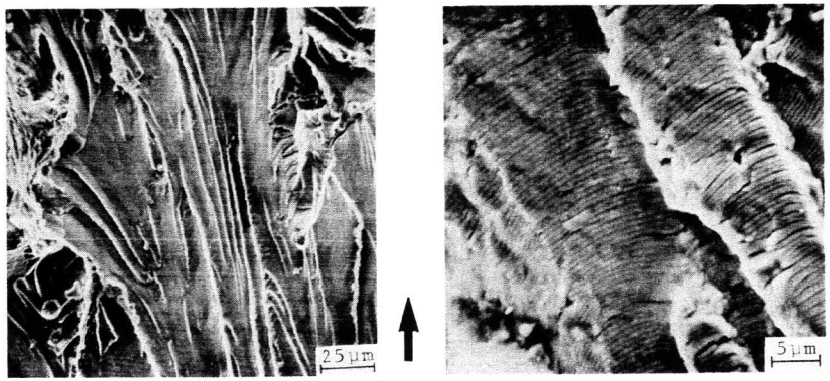

(a) (b)

Fig. 5. SEM fractographs
a) T-L in air, c.g.r. $\approx 2 \times 10^{-4}$ mm/cycle
b) T-L in air, c.g.r. $\approx 8 \times 10^{-4}$ mm/cycle
Arrow shows the crack growth direction.

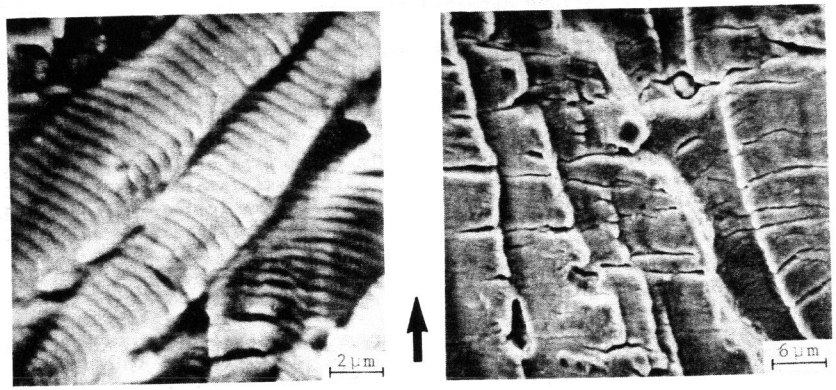

(a) (b)

Fig. 6. SEM fractographs
a) S-T in salt water fog, c.g.r. $\approx 7 \times 10^{-4}$ mm/cycle
b) T-S in air, c.g.r. $\approx 4 \times 10^{-4}$ mm/cycle
Arrow shows the crack growth direction.

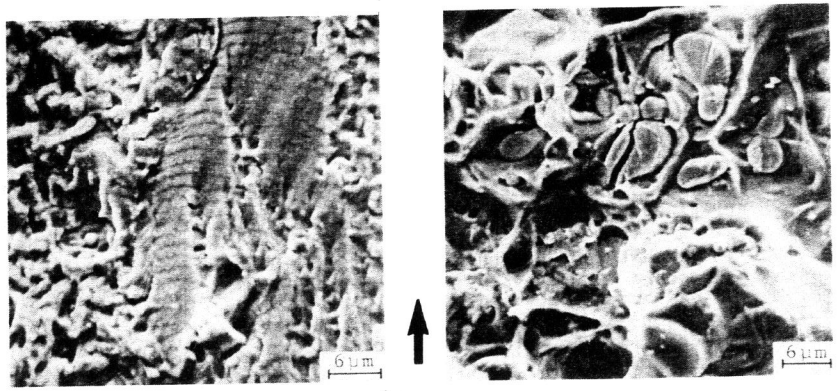

(a) (b)

Fig. 7. SEM fractographs
a) T-L in salt water fog, c.g.r. $\approx 2 \times 10^{-3}$ mm/cycle
b) T-S in salt water fog
Arrow shows the crack growth direction.

striations by deepening of the valley portions of striations. Fig. 4b shows the fatigue striations detected in a large secondary crack.

Particles of intermetallic compounds (probably $MgZn_2$) are observed in some regions of the fracture surfaces. Cracks usually cut those particles as seen in Fig. 7b in regions without striations and especially at low and medium crack growth rates.

Cracks, on the other hand, do not cut the particles in striated regions, but instead pass around them as can be seen in Figs. 3a and 4a. This phenomenon may be explained by the hydrogen diffusion around these particles causing the formation of micro-cracks at some distance from the crack tip.

CONCLUSIONS

1. Crack propagation is of transgranular type and occurs with several local fronts on different growth planes separated by tear ridges.
2. Fatigue striations are present extensively on crack propagation regions of the fracture surfaces. The density of striations decreases with increasing crack growth rates.
3. The random formation of striations around intermetallic particles can be explained by the existence of hydrogen embrittlement mechanism ahead of the crack tip. The diffused hydrogen at some distance from the crack tip is trapped around the particles forming microcracks that may propagate in any direction if the local stresses at these regions are high enough.
4. Many secondary cracks are found to be present on fatigue fracture surfaces. They are observed to coincide mostly with striations penetrating normal to the main fracture surface.

ACKNOWLEDGEMENT

This study is a part of a research carried out within the framework of the AGARD Additional Support Programme to South-Flank NATO Countries. The authors wish to express their thanks to the Structure and Materials Panel of AGARD for support of this research work.

REFERENCES

ASTM (1980). Standart test method for constant-load-amplitude fatigue crack growth rates above 10^{-8} m/cycle. Annual Book of ASTM Standarts, Designation E 647-78T, Part 10, 749-762.

Duquette, D.J. (1982). Mechanism of corrosion fatigue of aluminum alloys. AGARD Conference Proceedings No:316, Corrosion Fatigue, 1·1-1·12.

Gürbüz, R. (1987). Effect of orientation on salt water fog enhanced fatigue crack growth behavior of 7050 T73651 aluminum alloy. Ph.D. Thesis in Met. Eng., METU.

IABG (1976). Bauteilspezifische Werkstoffuntersuchungen, Untersuchungen an Halbzeug 7050-T73651, Bruchzahigkeit und Ermüdungssverhalten. Bericht Nr. TF-621·3.

Suresh, S., A.K. Vasudevan and P.E. Bretz (1984). Mechanisms of slow fatigue crack growth in high strength aluminum alloys: role of microstructure and environment. Metallurgical Transactions A, 15A, 369-379.